Experimental and Numerical Simulation of Girth Welded Joints of Dissimilar Metals in Clad Pipes

Author Name(s): Bridget Kogo[*], Bin Wang[*], Luiz Wrobel[*] and Mahmoud Chizari[*,♣]

[*]Mechanical, Aerospace and Civil Engineering, Brunel University London
Uxbridge, Middlesex, United Kingdom
[*,♣]School of Mechanical Engineering, Sharif University of Technology, Tehran, Iran

ABSTRACT

Welding of two dissimilar materials was carried out in-house with the aid of a Tungsten Arc weld having dynamic measurement of temperature profiles in the vicinity areas of the welding track using high temperature thermocouples. Comparison was shown previously of the simulated and measured transient temperatures versus finite element simulation. Stress analyses of the pipe were carried out using FEA simulations with two different clad thicknesses. Results of thermal analysis showed a close match and laboratory tests revealed the occurrences at the welded joints, FZ and HAZ; the result of stress analysis also showed a good agreement when validated with ND experimental results.

KEY WORDS: Thermal Analysis; Dissimilar Metals; Girth Welding; Clad Pipes; 3D Finite Element Modeling; HAZ; FZ

NOMENCLATURE

BC Boundary Condition
CES College of Engineering and Science
CM Clad Metal
FEA Finite Element Analysis
FZ Fusion Zone
GMAW Gas Metal Arc Weld
HAZ Heat Affected Zone
MS Mild Steel
ND Neutron Diffraction
PM Parent Metal
WA Weld Axis
WE Weld Edge
WL Weld Line
WM Weld Metal
WS Weld Start
SS Stainless Steel
TC Thermocouples

INTRODUCTION

The In joining technology, welding is one of the vital techniques used to make continuous pipelines in industry. The thermal and mechanical loading in the process has a profound impact on the integrity of the pipeline over its service life. An accurate and thorough assessment is needed on the associated residual stress and its effect on the structural properties of the pipeline.

One of the novelties of this research is the understanding of the temperature responses from the welded joints, demonstrated by positioning high temperature thermocouples at strategic points on the welded joints in order to capture the transient temperature response at different points. It is not enough to assume that the distribution of heat through the weld metal will depend on the distance from the thermocouples to the heat source only, but to actually study the temperature profile in order to uncover any peculiar trends.

The second impact of this research is the treatment of dissimilar materials through the implementation of a cladded layer. Previous experimental works have been carried out on the welding of single layer pipes, but very little work has been carried out on cladding. Cladding is carried out mainly for the purpose of increased strength after which other qualities like enhance corrosion resistance can follow. Since two metals of different chemical constituents are welded together, we study the properties of the newly formed weld joint in terms of its chemical composition, strength, corrosion resistance, etc. (Materia, 2006; Kah et al., 2014).

The Heat Affected Zone (HAZ) is also an impact as it addresses a gap in knowledge. Since welding is carried out on two dissimilar materials, there is the need to investigate what occurs in the HAZ of the welded joint since the chemical component of the HAZ is altered via high weld temperatures. There is also a need to understand the location of the weakest point of burst because if a structure is to fail, the failure begins at that point.

The thermal properties of the inner and outer surfaces of the pipe have been clearly defined and described in the paper. The FEA software has considered the transient temperature variations and has obtained close agreement with the experiment. It has been noted that the friction between the two layers has not been considered – we defined a frictionless contact between the two layers because we considered the relative motion between the two layers to be negligible; friction, however, can be considered in future research.

The thermal analysis in cladded girth welded joints has been carried out using 3D finite element analysis in Abaqus. Results of the transient temperature curves have been generated for the different cladding thicknesses (stainless steel and mild steel).

Welding of the two dissimilar materials was also carried out in-house with the aid of a Tungsten Arc weld with dynamic measurement of temperature profile in the vicinity areas of the welding track using high temperature thermocouples. Comparison of the measured temperature versus the simulation outcome shows good agreement. Laboratory tests were also carried out to reveal the occurrences at the Fusion Zone (FZ) and the HAZ of the welded joints.

In the thermal model, it was observed that the distribution of heat in the HAZ was maximum at the heat source position and minimum at the start and end points, indicating that heat was trapped in the middle region which is responsible for the fluctuations in the heat distribution

in these zones (Inspectioneering, 2016). It has therefore been deduced that the heat was retained within the welding spool for approximately 10 seconds in the middle region of the weld prior to cooling. The distribution was also considered in the final output as a result of the cavities present within the model (Lampman, 2001; Goldak, 2005; Youtsos, 2006; Muhammad, 2008).

Convection is the major procedure for transmission of heat from the weld strip to the immediate environment, whereas the radiation boundary condition has minimal or no consequence on the estimated temperatures and could be overlooked.

The findings of this research help to provide a better understanding of the thermal loading occurring in the welding of two dissimilar materials, and contributes to the effort to enhance the performance of clad pipelines in service.

WELD PARAMETERS

Thermal and mechanical material properties of stainless steel as tabulated in Brickstad and Josefson (1998) and presented in graphical form by Yaghi et al. (2006) combined a set of material properties plotted against temperature on a single graph. Young's modulus E decreased with increasing temperature, whereas the thermal conductivity λ increases with increases in temperature. The heat capacity C also increases with increases in temperature until it gets to the peak at a temperature of 1400°C, when the stainless steel melts, after which it remains constant. The phase dissolution temperatures for the parent metal as well as the weld metal decrease with respect to increasing temperature. The thermal coefficient of expansion α is constant. Kinematic hardening was applied in both the thermal and stress analyses of the finite element modelling. The material density is 7,850kg/m³ for carbon steel and 7,970kg/m³ for stainless steel. The liquidus temperature employed here is 1400°C for both the stainless steel and the mild steel. The solidus temperature is 1,375 °C. The latent heat capacity of 260kJ/kg was utilized (Yaghi et al., 2006).

The respective material properties used in the FEA analysis were sourced from the College of Engineering and Sciences (CES) Edu Pack 2016 Version: 16.1.22 - Granta Design Limited, Cambridge CB1 7EG, United Kingdom.

GEOMETRY OF THE MODEL

FEA simulations of both thermal and stress analysis were carried out using Abaqus ver.2016 (Dassault Systèmes) using a 3D pipe geometry measuring 160mm length, 10mm thickness for carbon steel and 2mm or 12mm thickness for stainless steel, respectively. Figure 1 shows a typical pipe model with the line of axis along the middle and the parent metal, as well as the clad metal, clearly labelled.

For the fully cladded pipe shown in Figure 1, the element type for the stress analysis is the 10-node quadratic tetrahedron C3D10 with a total of 222,449 nodes and 148,918 elements, whereas the element used for the thermal analysis is the C3D10 quadratic heat transfer tetrahedron with a total number of 157,519 elements and 233,600 nodes as shown in Figure 2. The family for the stress analysis is 3D Stress and element library is standard. It has a quadratic geometric order.

The Tetrahedron element was chosen because of its very good meshing facilities including multifaceted geometries. FEA thermal loads and boundary conditions for the simulation of a multipass welding thermal cycle are heat losses from the surface via convection and radiation. The difference in the amount of heat inputted in each pass is accounted for and this corresponds to the time taken to weld, as well as the waiting time before the start of each subsequent pass (Pathak et al., 2012).

GAS METAL ARC WELD

The Gaussian transformation principle states that a Gaussian flat surface has a Gaussian curvature at each and every point of the magnitude of zero (Kogo et al., 2017a). In other words, provided the dimensions are consistent, a plate can be transformed into a pipe and vice-versa. Going by this principle, the surface of a cylinder can be said to be a Gaussian flat plane since it can be revolved from a piece of paper. Furthermore, the implication is that this can be done without stretching the plane, folding or tearing it. The parameter r(u,v) is an orthogonal parameterization of a surface (Bhatia, 2014; EDU, 2016).

A mild steel plate of thickness 10mm and dimension 150mm by 100 mm of grade CR4 was mounted on a stainless steel 316 grade plate, 2mm thick, of dimension 150mm by 100mm, and butt welded with a 60 degree V-groove for butt welding. This was used in the first set of weld experiments (Kogo et al. 2017b).

For the second set of weld experiments, a mild steel plate of thickness 10mm and dimension 75mm by 100 mm of grade CR4 was mounted on a stainless steel 316 grade plate 12mm thick of dimension 75mm by 100mm and butt welded with a 50 degree V-groove, see Figures 4 to
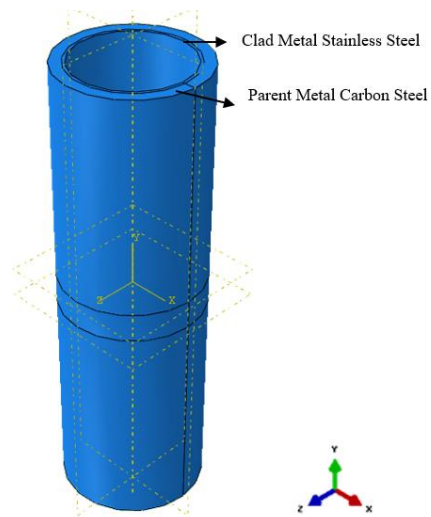

Fig. 1 Geometry and weld line of full pipe model.

The respective distances of the thermocouple from the weld edge (WE), weld line (WL), weld start axis (WSA) and weld start (WS) positions shown in Figures 4 and 5 are measured, as well as the time taken to attain the peak transient temperature values. The transient temperature curves for the 2mm clad and the 12mm clad thicknesses were obtained (Kogo et al., 2017b).

Fig. 2 (a) Full cladded pipe showing quadratic tetrahedral elements of type C3D10 (b) Cross-section of pipe mesh showing clad metal and parent metal.
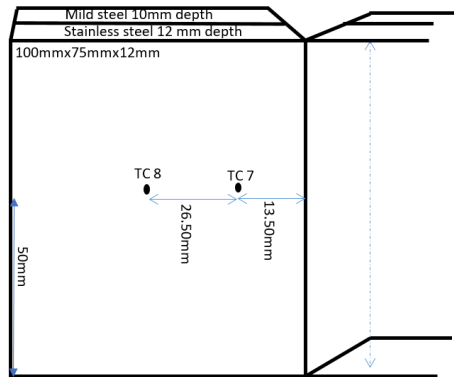

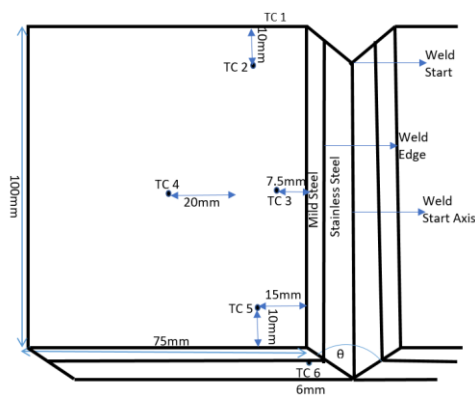Fig. 3. Bottom view of weld plan and thermocouple positions TC7 & TC8.

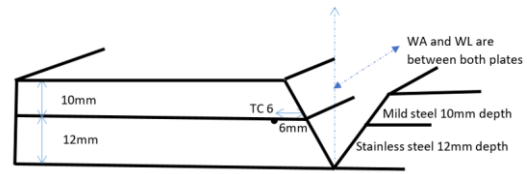Fig. 4 Top view of weld plan and thermocouple positions TC1 – TC6.

Fig. 5 Side view of weld plan and thermocouple positions TC6.

High temperature thermocouples were spot-welded to specific positions on the carbon steel and stainless steel plates, and each terminal fed into a Pico logger, which subsequently transmitted the temperature responses from the thermocouples into transient temperature profiles displayed on the monitor of a laptop. Thermocouples, TC1 to TC 6 were placed on the 2mm MSSS cladded plates, while thermocouples TC1 to TC8 were placed on the 12mm MSSS cladded plates illustrated in Figures 3 to 5.

THERMAL RESPONSES OF THERMOCOUPLES

Transient temperature curves were obtained from the thermal analysis discussed in previous paper (Kogo et al., 2017b). Thermocouple TC7 was first to receive the heat signal and depicted a thermal peak irrespective of its position (50mm) away from the heat source and beneath the weld array Figure 3, considering the thermal conductivity of stainless steel, which is 16 W/mK; however, TC1 placed 13.5mm attained the highest temperature peak much later than TC7 and TC2 (placed 15mm from WE) on weld array shown in Figure 4. On the 2mm thickness array, TC5 positioned at 50mm from Heat source and beneath the weld attains thermal peak before TC2, which is positioned 50mm from the heat source by reason of thermal conductivity of steel. TC2 traps the heat and slowly dissipates it to the surrounding thermocouples.

THERMAL ANALYSIS

Hot Passes

In this research, a weld bead is referred to as a pass. There are seven passes for the 3D weld models and the different thickness of clads for the 3D simulated models. This is regarded as good practice to simplify weld models by representing several weld beads by a pass. For simplicity, it is also assumed that the first weld bead is laid prior to the next and so on until the final weld bead, the seventh pass, is completed. The weld bead is represented in (Kogo et al, 2017b). This weld profile clearly illustrates the temperature profile of the weld pass 1 at different increments and time steps along the path line of the weld, at constant speed. The temperature distribution varies for the different time steps and weld increments, irrespective of the fact that it is the same weld pass. The different colour bands represent the different zones within the weld region. The FZ has colour bands red to orange, while the HAZ is yellow to light blue and the PM is dark blue.

Cold Passes

The cold passes for the ring added mass in the cylinder are shown in Figure 6. It is important to note that the temperature range is almost the same in the cooling phase and this ranges from 836 °C to 652 °C, with a difference of 184 °C. The different colour bands correspond to different temperature profiles which represent the FZ, the HAZ and the rest of the pipe. Similarly, the FZ is depicted by the red-orange colour band which corresponds to 803 °C to 836 °C whereas the HAZs lie within the

colour band yellow to greenish blue. These are the 658 ℃ to 787 ℃ bands, leaving the rest of the pipe at a temperature of 642 ℃ for further cooling to occur.
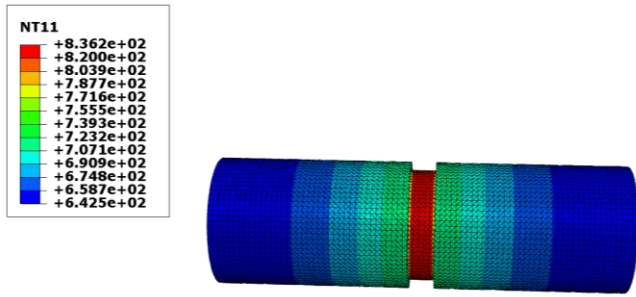

Fig. 6 Complete thermal model of a fully cladded pipe, cool pass 7 at increment 10, time step 3,600 seconds.

STRESS ANALYSIS

RESIDUAL AXIAL STRESS

Consider the residual stress along the S13 direction (that is the Y-axis) as depicted by the arrow in the FEA simulation in Figure 7; the axial (longitudinal) stress across the length of the pipe is shown in the graph. This depicts a maximum value of 378MPa which is agreement with the yield stress of 378 MPa and 400 MPa. It can also be further compared with the residual stress analysis of the outer pipe carried out by Sinha et al. (2013).

Deformation refers to an alteration in the size or shape of an object as a result of application of energy; in this case, heat is transferred. In some other cases, the forces could be mechanical and sourced by compressive forces or pushing, torsion or bending forces and shear or even tensile forces responsible for pushing.

In the thermal analysis, heat is being applied to the body, pipes and plates, resulting in mobility of grain boundaries, line and screw dislocations, point vacancies, stacking faults and twins in both crystalline and non-crystalline solids. The displacement of these defects is triggered thermally hence hindering the rate of atomic diffusion.

For deformation to occur, intermolecular forces within an object or body resists such external forces; and if the internal forces is great, the body assumes a new state of equilibrium and returns back to its original shape. If the applied forces overcome the internal forces, deformation sets in.

For the fully cladded pipe shown in Figure 7, the element type is C3D10, a 10-node quadratic tetrahedron with a total of 222,449 nodes and 148,918 elements. An element of type C3D10 is a 10 node quadratic tetrahedron.
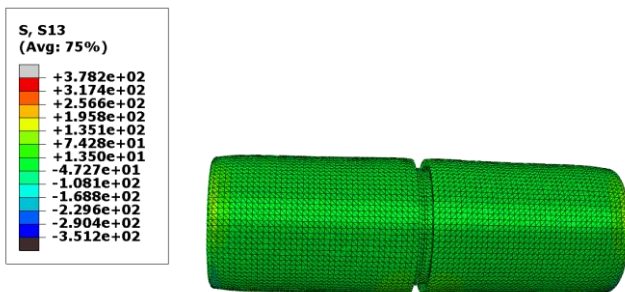

Fig. 7 Pipe Model showing stress in the S13 direction

WELD DIRECTION (NOMENCLATURE)

It is important to note here that the direction considered when taking the readings from the pipes is the clockwise direction, with the first reading taken from angle 45 degrees as illustrated in Figure 8 and explained under this section. Some researchers conventionally take to the 90º, 180º, 270 º and 360 º angles, also connoted as 3 O'clock, 6 O'clock, 9 O'clock and 12 O'clock convention. This is the order in which the axial stresses were taken.
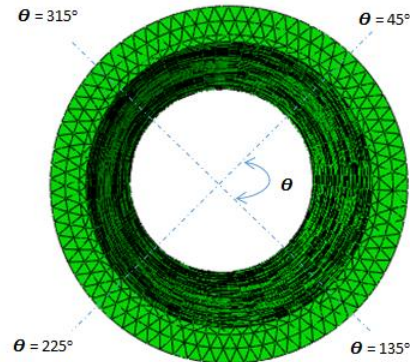

Fig. 8 Cross section view of the pipe circumference illustrating the order of weld direction

Analysis of Residual Axial Stress Result

It can be seen from Figure 10 for the residual axial stress in the cladded pipe that close to the weld vicinity, compressive and tensile stress fields are present in and near the section of the weld, both on the external and internal surfaces of the pipe. Furthermore, this occurrence can be credited to the varying temperature profiles without and within the surfaces of the pipe. Because of the thickness of the wall of the cylinder and very close to the weld line (which is represented by the vertical line), the tensile and compressive residual stress field are generated due to shrinkage occurring within the weld pipe. The findings in Figure 10 are similar to that in Sinha et al (2013) and Dar et al (2009).

The differences in the values of the residual stresses are a result of the different material properties such as yield strength for the base and filler metals, weld geometry and heat source parameters. There have been volumetric change and yield strength as seen under tensile test curves (Kogo et al, 2017b), as a result of martensitic transformation which have effects on the welding residual stress, by increasing the magnitude of the residual stress in the weld zone as well as changing its sign. The simulated results show that the volumetric change and the yield strength change due to martensitic transformation (Kogo et al, 2017c), and these have influences on the welding residual stress.

NARROW GAP WELDING

Part of this research was carried out in collaboration with the National Structural Integrity Research Centre (NSIRC) based at The Welding Institute (TWI) in Cambridge, UK. Experiments using narrow gap welding, otherwise known as narrow grove welding, was employed using varying angles from 2-20º. This is a recent welding technique which represents an economically viable means of welding thick pipe sections as it involves a smaller amount of weld metal and welding times.
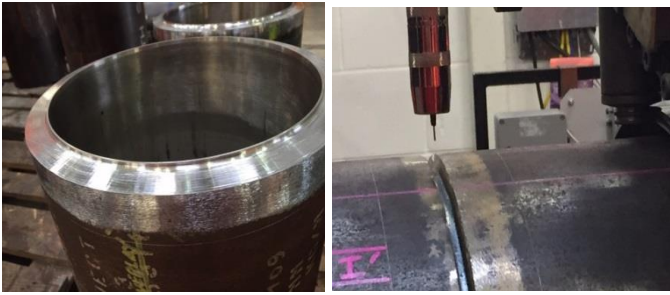
Fig. 9 (a) Narrow gap welding in SubSea 7 Lab – Pipe edges cleaned showing and (b) Narrow gap weld in SubSea 7 Lab

Narrow gap welding of subsea pipelines was carried out at the Standard Laboratory in Subsea 7, Glasgow, Scotland with NSIRC's collaboration. Standard hygiene and welding laboratory regulations were strictly adhered at a temperature of 1500ºC and forty-eight thermocouples used alongside forty-eight strain gauges. The sets of data obtained from this experiment were used to validate the findings from the stress model.

RESULTS AND DISCUSSIONS

Tensile stresses are symmetric across the weld line, in and around the FZ and the HAZ. A high stress field can be seen on the inner surface of pipe. Compressive stresses are also symmetric across weld line, with a high stress field on the outer surface of pipe.
A protuberance (hump-like) is present in the profile at the outer surface of pipe within the region of the weld line, indicating the existence of stress variation underneath the weld crown. A region of high stress can be seen within the HAZ.

Figure 10 and 11 showing residual axial stresses versus distance curves for the 2 mm clad pipes
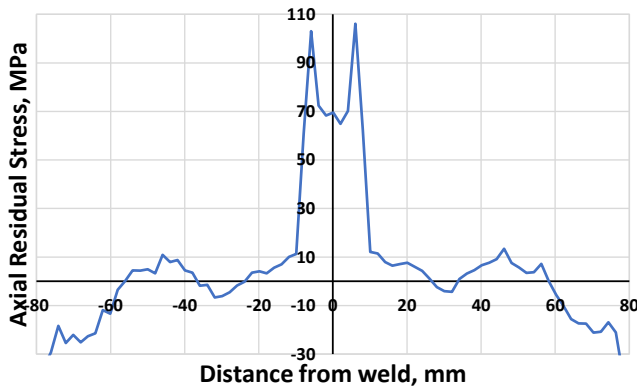

Fig. 10 Residual axial stresses versus distance curve for the inner surface of the 2 mm clad pipes
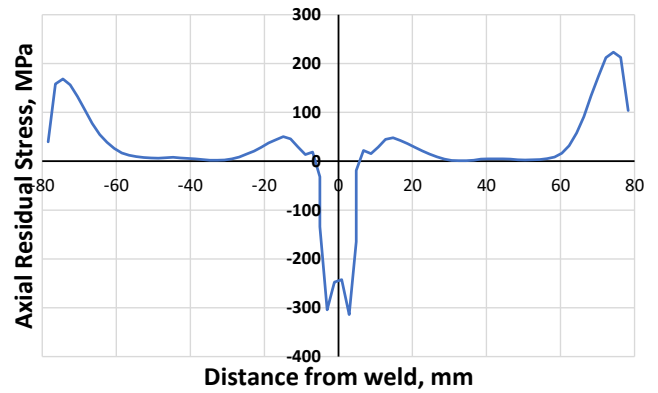

Fig. 11 Residual axial stresses versus distance curve for the outer surface of the 2 mm clad pipes

Figure 12 and 13 showing residual axial stresses versus distance curves for the 12 mm clad pipes
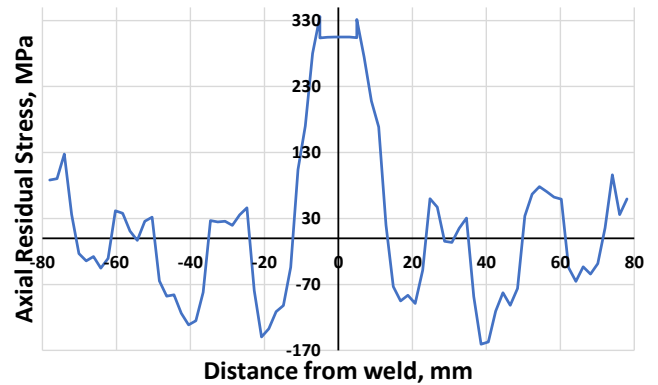

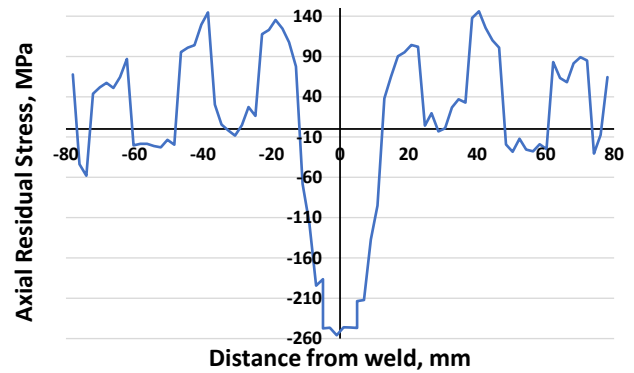Fig. 12 Residual axial stresses (average value) on the inner surface of the HAZ of the 12 mm clad pipes

Fig 13 Residual axial stresses (average value) versus distance curve on the outer surface of the HAZ of the 12 mm clad pipes

Neutron Diffraction (ND) Measured Stress Curve

Being part of a team involved in carrying out Narrow Gap Weld experiment and measurement at subsea 7 standard laboratory in Glasgow, the ND measured stress was carried out and here is the curve obtained from the weld measurement. The Residual, Axial and Hoop

stress measurement are displayed below. Residual Axial Stress on the inside of the pipe with outer diameter of 14-inch, wall thickness of 19.05mm and a length of 750mm.

Fig. 14 Narrow Gap weld in SubSea 7 Lab joining of both pipes

The narrow gap weld is carried out on a revolving work piece and consists of a straight single pass applied layer after layer. The weld procedure demands that both the operating weldability and weld shrinkage must be taken into account.

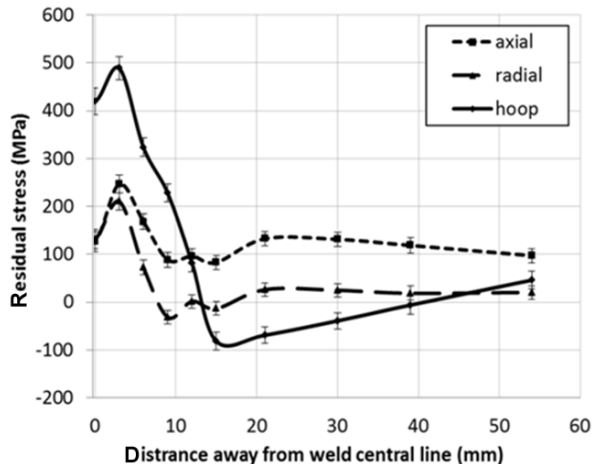A typical ND measured stress showing the stress distributions is shown in Figure 15

Fig. 15 A typical Neutron Diffraction (ND) measured stress showing the residual axial, radial and hoop stress distributions on the subsurface of pipe

Observations:
Close to the weld region comprehensive axial, radial and hoop stresses can be observed but farther away from the weld region, tensile stresses become the trend. Because of the symmetry across the weld line the axial, radial and hoop stresses are symmetric in nature.

The thermal cycles generated from the weld whose setup is shown in Figures 3-5 clearly portray the fact that the temperature at a specific point reaches a maximum with respect to time when the weld torch crosses a corresponding section of the weld, and the agreement is very good for the maximum temperatures.

The nature of the material used in the modelling of the weld parameters play a very significant role in the temperature – time displacement curve. The nature of the actual material used is another reason for the lag observed in the curve for the measured data.

Recall that in the measured data generated from the weld set-up in

Figures 3 to 5, the thermocouples did detect heat at different rates at different times, and only attained peak values when the heat source was right at the same spot as the thermocouples. This clearly means that the response to temperature was dependent on several factors, such as the nature of the material (stainless steel or mild steel), material thickness (depth, height and width), thermal conductivity of the material (steel is 16 W/mK and mild steel is 36 W/mK), distance from the heat source and time of transmission (time at which the temperature reading is taken), all of which affect the temperature-time curve displayed in the figures. The peak is highest for the 2mm SS clad than in the 12mm SS clad.

CONCLUSIONS

An experimental study has been carried out on GMAW of two different clad thicknesses, 2mm and 12mm, using high temperature thermocouples and the transient temperature responses obtained. An FEA model has also been developed using the Abaqus software and the transient temperature curves and residual stress curves were obtained. The following conclusions were arrived at:

1. Comparison of the measured with the simulated results reveals a very good agreement, which validates the FEA model used.
2. The result of the mechanical tests reveals that the weakest point in the welded joints of both 2mm clad thickness and 12mm clad thickness is the HAZ, due to ductile to brittle fracture as well as martensitic distortion.
3. Because of the symmetry across the weld line, the axial stresses are symmetric in nature, that is compressive stresses which are high in magnitude are observed outside the pipe surfaces while tensile stresses are seen inside the pipe surfaces.
4. The circumferential position of the weld bead does not determine or affect the axial stresses. This is seen from the fact that the distribution of the axial stresses in and outside the pipe are similar in magnitude and distribution.
5. A protuberance (hump-like shape) is seen at the exterior surface of the pipe close to the weld line which shows the distribution of the stress variation under the weld crown.

From the results of the axial stresses and the typical ND measured stresses showing the residual axial, radial and hoop stress distributions on the inner surface of pipe, the following can be concluded:

6. Close to the region of weld comprehensive axial, radial and hoop stresses are observed but farther away from the weld region, tensile stresses become the trend.
7. Also, because of the symmetry across the weld line, the axial, radial and hoop stresses are symmetric in nature.
8. The result of the ND measured stress experiment at the Subsea 7 laboratories further confirms the validity of the simulation carried out in this research.

ACKNOWLEDGEMENTS

REFERENCES

Bhatia, A. (2014, September 5). Curvature. Retrieved December 29, 2016, from Empirical Zeal: http://www.empiricalzeal.com/tag/curvature/

Brickstad, B. and Josefson, B.L. (1998) A Parametric Study of Residual Stresses in Multi-Pass Butt-Welded Stainless Steel Pipes, *International Journal of Pressure Vessels and Piping*, Vol. 75, 11-25.

Dar, N. U.; Qureshi, E. M. and Hammouda, M.M.I. (2009). Analysis of Weld-Induced Residual Stresses and Distortions in Thin-Walled Cylinders. *Journal of Mechanical Science and Technology*, Vol. 23, 1118-1131.

EDU, M. E. (n.d.). Guassian Curvature. Retrieved December 29, 2016, from Math ETSU EDU: http://math.etsu.edu/multicalc/prealpha/Chap3/Chap3-8/part3.htmGoldak, J. A. (2005). *Computational Welding Mechanics.* New York: Springer.

Goldak, J. A. (2005). *Computational Welding Mechanics.* New York: Springer.

Inspectioneering. (2016, June 21). *Heat Affected Zone (HAZ).* Retrieved October 03, 2016, from Inspectioneering : https://inspectioneering.com/tag/heat+affected+zone

(IJRTE), 2277-3878.

Yaghi, A.; Hyde, T. H.; Becker, A. A.; Sun, W. and Williams J. A. (2006). Residual Stress Simulation in Thin and Thick-Walled Stainless Steel Pipe Welds Including Pipe Diameter Effects.

Kah, P., Shrestha, M. and Martikainen, J. (2014). Trends in Joining Dissimilar Metals by Welding. *Applied Mechanics and Materials*, Vol. 440, 269-276.

Kogo, B., Wang, B., Wrobel, L. and Chizari M. (2017a). Residual Stress Simulations of Girth Welding in Subsea Pipelines. Proceedings of the World Congress on Engineering 2017, Vol II (pp. 1-6). London, U.K.

Kogo, B. Wang, B. Wrobel, L. and Chizari, M., (2017b). Analysis of Girth Welded Joints of Dissimilar Metals in Clad Pipes: Experimental and Numerical Analysis. Proceedings of the Twenty-Seventh International Society of Ocean and Polar Engineering Conference, San Francisco, CA, USA.

Kogo, B. Wang, B., Wrobel, L. and Chizari, M. (2018). Microstructural Analysis of a Girth Welded Subsea Pipe . *Engineering Letters, 26:1, EL_26_1_23*, 1-10, pp. 193-200.

Lampman, S. (2001). *Weld Integrity and Performance.* Ohio: ASM International.

Materia, T. (2006). *Welding of Dissimilar Metals.* Retrieved October 04, 2016, from Total Materia: http://www.totalmateria.com/page.aspx?ID=CheckArticle&site=ktn&NM=15

Muhammad, E. (2008). *Analysis of Residual Stresses and Distortions in Circumferentially Welded Thin-Walled Cylinders.* Parkistan: National University of Science and Technology, Parkistan.

Pathak, C.S.; Navale, L., G.; Sahasrabudhe, A. D. and Rathod, M. J. (2012). Analysis of Thermal Cycle during Multipass Arc Welding. *Welding Journal*, Vol. 91, 149-154.

Sinha, P. K., Islam, R. and Prasad, C. A. (2013). Analysis of Residual Stresses and Distortions in Girth-Welded Carbon Steel Pipe. *International Journal of Recent Technology and Engineering*

International Journal of Pressure Vessels and Piping, Vol. 83, 864-874.

Youtsos, A. G. (2006). *Residual Stress and its Effects on Fatigue and Fracture.* Dordrecht, The Netherlands: Springer.